Available online at www.sciencedirect.com
ScienceDirect
Journal of the European Ceramic Society 30 (2010) 981–991
www.elsevier.com/locate/jeurceramsoc

Phase evolution in reaction sintered zirconium titanate based materials

E. López-López [a], M.L. Sanjuán [b], R. Moreno [a], C. Baudín [a,*]

[a] *Instituto de Cerámica y Vidrio (CSIC), C/Kelsen 5, 28049 Madrid, Spain*
[b] *Instituto de Ciencia de Materiales de Aragón (CSIC), Facultad de Ciencias, Universidad de Zaragoza, 50009 Zaragoza, Spain*

Received 5 March 2009; received in revised form 6 October 2009; accepted 20 October 2009
Available online 22 November 2009

Abstract

Zirconium titanate materials are proposed for structural components for which fully reacted and relatively large pieces are required. In this work the phase evolution in slip cast compacts constituted by equimolar mixtures of TiO_2 and ZrO_2 stabilized with 3 mol% of Y_2O_3 at high temperature is studied, to establish the basis to design suitable thermal treatments for $ZrO_2(Y_2O_3)$–TiO_2 materials. The temperatures at which the processes involved in the reaction sintering occurred were identified by constant heating rate experiments. Phase and microstructure analyses have been performed on specimens treated at the identified temperatures and air quenched. Then the adequate temperature range to get fully reacted and dense materials has been deduced. Materials treated at 1500 °C to 2 h were constituted by $Zr_5Ti_7O_{24}$ as major phase, a solid solution of TiO_2 and Y_2O_3 in c-ZrO_2 as secondary phase and a ZrO_2–TiO_2–Y_2O_3 non-stoichiometric compound with pyrochlore structure as minor phase. Pyrochlore was demonstrated to be a metastable phase at 1500 °C.

Keywords: Sintering; Microstructure-final; ZrO_2; TiO_2; Zirconium titanate

1. Introduction

The stoichiometric zirconium titanate, $ZrTiO_4$, presents crystallographic anisotropy in thermal expansion ($\alpha_{a25–800\,^\circ C} = 6.2 \times 10^{-6}\,^\circ C^{-1}$, $\alpha_{b25–800\,^\circ C} = 10 \times 10^{-6}\,^\circ C^{-1}$, $\alpha_{c25–800\,^\circ C} = 8.6 \times 10^{-6}\,^\circ C^{-1}$[11])[b] and, therefore, it has high potential as constituent of low thermal expansion materials for structural applications. Thus, the fabrication of relatively large bulk pieces would be required. A main problem of the materials whose low thermal expansion derives from anisotropy is that it is usually associated to extensive microcracking. In this sense, it would be desirable to count with a phase compatible with zirconium titanate such as a zirconia polymorph, to add as reinforcing second phase for which the possibility of obtaining materials in the ZrO_2–TiO_2–Y_2O_3 system would be adequate. As discussed below, the composition and structure of zirconium titanate are variable as a function of the experimental parameters used to obtain the material. Moreover, there is no general agreement on the phase equilibrium relationships in the ZrO_2–TiO_2–Y_2O_3 system. Therefore, the study of the phase development in zirconium titanate based materials is required.

The formation of $ZrTiO_4$ has been studied by several authors.[2–10] Although it is possible to obtain $ZrTiO_4$ at temperatures around 600 °C by sol–gel methods,[2] the solid state reaction from the oxides of zirconium and titanium is required for the fabrication of relatively large bulk pieces. According to calculations by Hom et al.[3] the formation of $ZrTiO_4$ from the oxides is thermodynamically favourable from about 980 °C (1250 ± 150 K), however, it has only been reported at temperatures between 1300 and 1600 °C.[3–10] The stoichiometric zirconium titanate ($ZrTiO_4$) is the stable phase at high temperature (>1200 °C),[9] whereas, for lower temperatures (<1100 °C) the composition of zirconium titanate shifts towards higher TiO_2 contents. McHale and Roth,[9] after annealing compacts with the stoichiometric composition ($ZrTiO_4$) at 1000 °C for more than 4 months, concluded that the composition of the stable phase of zirconium titanate below 1100 °C was $ZrTi_2O_6$. For lower annealing periods the obtained phase was $Zr_5Ti_7O_{24}$.[9,11] For relatively short thermal treatments such as those used in ceramic processing, $Zr_5Ti_7O_{24}$ is only formed in the presence of additives such as Y_2O_3.[12,13]

* Corresponding author. Tel.: +34 917355840; fax: +34 917355843.
E-mail address: cbaudin@icv.csic.es (C. Baudín).
[b] Lattice: orthorhombic. Space group: *Pnab*. $a = 5.03580$ nm, $b = 5.48740$ nm, and $c = 4.80180$ nm. ASTM 34-415.

0955-2219/$ – see front matter © 2009 Elsevier Ltd. All rights reserved.
doi:10.1016/j.jeurceramsoc.2009.10.012

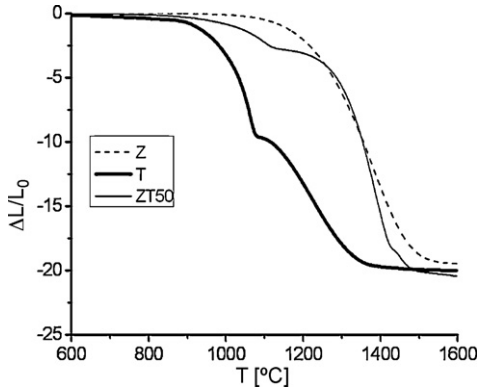

Fig. 1. Shrinkage versus temperature recorded during the heating part of the constant heating rate experiments (5 °C/min) for the studied compositions Y-TZP (Z), TiO_2 (T) and 50 mol% Z/50 mol% T (ZT50).

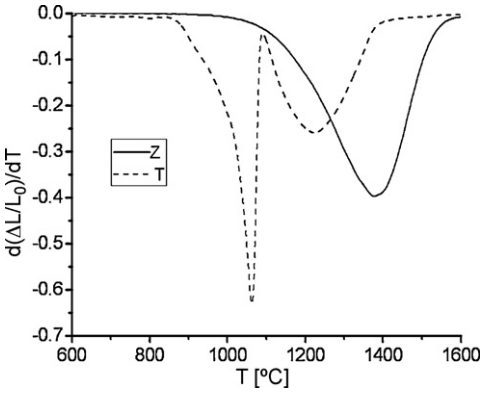

Fig. 2. Derivate versus temperature of the curves plotted in Fig. 1 for Z and T.

Although the complete ZrO_2–TiO_2–Y_2O_3 phase equilibrium diagram has not been yet established, some studies have been done.[14–18] On one hand, Fagg et al.[14] studied the solubility limits and transport properties of fluorite compounds with 10 and 12.5 mol% of Y_2O_3 in the system ZrO_2–TiO_2–Y_2O_3 demonstrating that the discrepancies among different data available in the literature are mainly related to fluctuations of temperature and/or cooling rates.

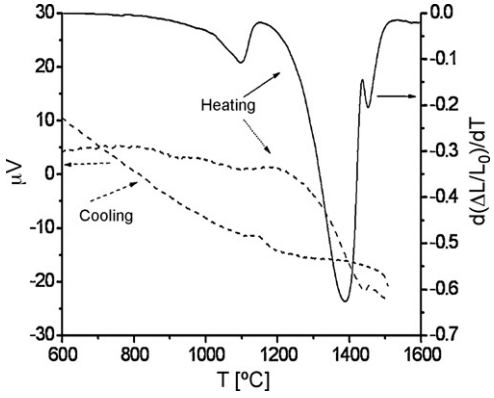

Fig. 3. Derivative versus temperature of the curve plotted in Fig. 1 for ZT50 together with the differential thermal analysis (DTA) curves recorded for heating and cooling during the constant heating rate experiments for ZT50.

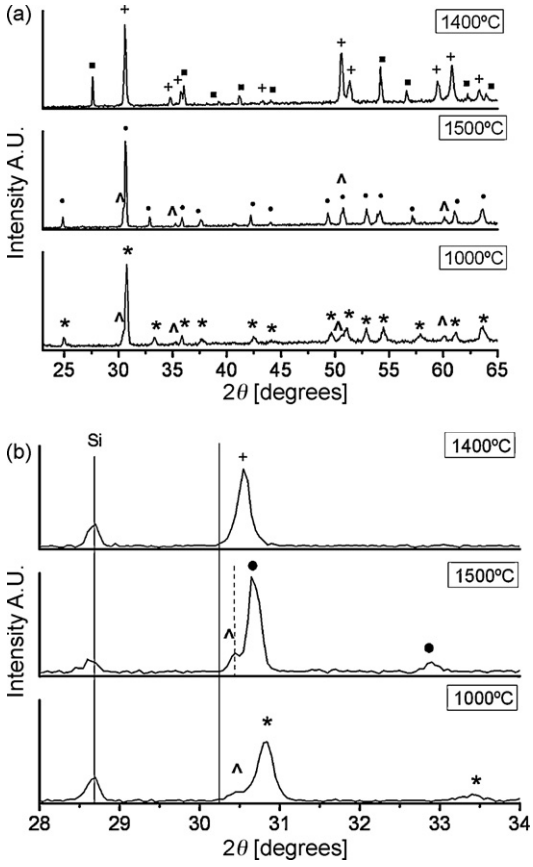

Fig. 4. X-ray diffraction spectra of ZT50 samples after quenching tests in air from 1400 and 1500 °C on heating and from 1000 °C on cooling. Si was used as internal standard. (*) $Zr_5Ti_7O_{24}$, (●) $ZrTiO_4$ss + t-ZrO_2ss, (■) r-TiO_2, (∧) c-ZrO_2ss. (a) General spectra and (b) detail of the spectra showing the shift of the zirconium titanate ($ZrTiO_4$ss) and the tetragonal zirconia (t-ZrO_2ss) peaks of the material from $ZrTiO_4$ (ASTM 34-415, dashed line) and $Zr_{0.963}Y_{0.037}O_{1.982}$ (ASTM 83-113, solid line), respectively.

On the other hand, several authors[15–18] studied this system proposing isothermal sections at 1500 °C, showing that for equimolar mixtures of TiO_2 and ZrO_2 and low Y_2O_3 contents (<1 mol%) the only stable phase would be zirconium titanate solid solution while for higher Y_2O_3 contents these studies predict different phases. Colomer[15] predicts a solid solubility limit of Y_2O_3 in zirconium titanate at 1500 °C about 3 mol%, being the compatible phases for higher Y_2O_3 amounts zirconium titanate and cubic zirconia. Schaedler[17] and Kobayashi[18] also predict these phases for compositions out of the region of Y_2O_3 solid solution in zirconium titanate but setting the limits of solubility of Y_2O_3 in zirconium titanate in ≈1 and ≈0.5 mol%, respectively. The compatible phases proposed by Feighery[16] out of the region of Y_2O_3 solid solution in zirconium titanate are pyrochlore and zirconium titanate, with a limit of solubility of Y_2O_3 in zirconium titanate of ≈1 mol%. According to Schaedler et al.,[17] the compatibility between zirconium titanate and pyrochlore is only possible at lower temperature (1300 °C).

However, there are no experimental data in the above mentioned studies that allow establishing the exact point for the solid solubility limit of Y_2O_3 in zirconium titanate at 1500 °C. Colomer et al.[15] focused the studies in the zirconia-rich region

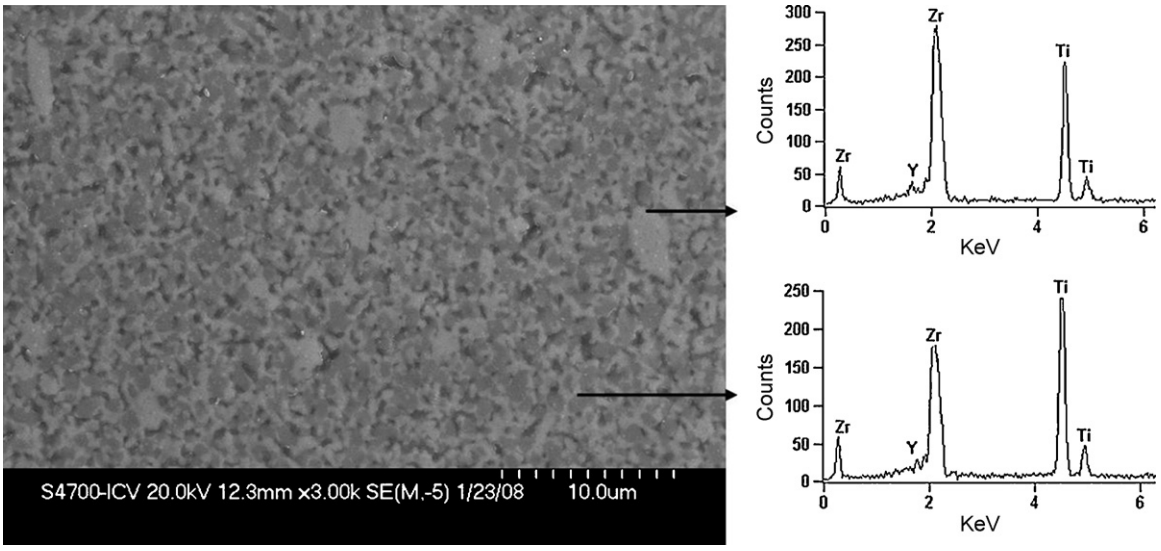

Fig. 5. Microstructure of ZT50 quenched from 1400 °C on heating. FE-SEM micrographs of polished surfaces, together with characteristic EDX analyses. Ti and Zr are the major components in the gray and white areas, respectively.

(65–97 mol%), the closest composition studied by Schaedler et al.[17] was 42.1 mol% ZrO_2, 52.6 mol% TiO_2, 5.3 mol% Y_2O_3, and the only compositions in the zirconium titanate primary field analysed by Feighery et al.[16] and Kobayashi et al.[18] were in the ZrO_2–TiO_2 binary system. The closest compositions studied by these authors are ≈54.5 mol% ZrO_2, ≈44.0 mol% TiO_2, ≈1.5 mol% Y_2O_3[16] and ≈48.0 mol% ZrO_2, ≈48.0 mol% TiO_2, ≈4.0 mol% Y_2O_3.[18] McHale and Roth[9] studied compositions with 0.5 mol% of Y_2O_3 and different contents of ZrO_2 (41.46–54.73 mol%) and TiO_2 (58.04–44.77 mol%) at 1500 °C for which zirconium titanate was the only phase.

In this context the objective of this work was to study the phase and microstructural evolution during reaction sintering of equimolar mixtures of TiO_2, and ZrO_2 stabilized with 3 mol% of Y_2O_3 (50 mol% TiO_2, 48.5 mol% ZrO_2, 1.5 mol% Y_2O_3), to establish the basis to design suitable thermal treatments for materials in the $ZrO_2(Y_2O_3)$–TiO_2 system. In a previous work the rheological behaviours of aqueous slips of the powders and their mixture were studied in order to establish the optimum processing conditions to get high green density bodies by casting of stable slips in plaster moulds.[19]

2. Experimental

Commercial ZrO_2 stabilized with 3 mol% of Y_2O_3 (yttria-tetragonal zirconia polycrystal Y-TZP, TZ3YS, TOSOH, Tokyo, Japan) and anatase-TiO_2 (Merck, 808, Darmstadt, Germany) were used as precursor powders. These powders have average particle diameters of 0.4 and 0.3 μm, respectively, and specific surface areas of 6.7 and 9.0 m^2/g, respectively.

The particle size distribution was determined with a laser diffraction analyser (Mastersizer S, Malvern, Worcestershire, United Kingdom), and the specific surface area was measured by the N_2 adsorption method (Monosorb Surface Area Analyser MS13, Quantachrome Co., FL, USA).

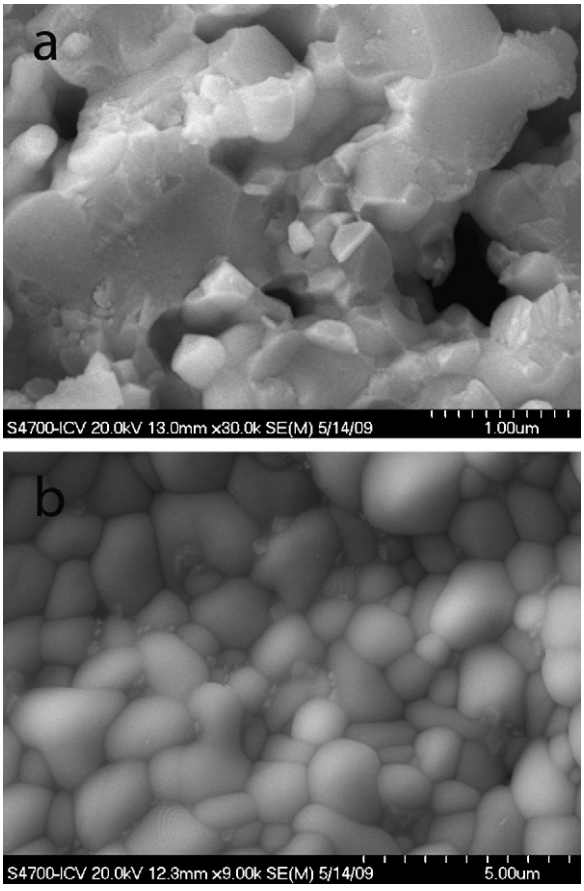

Fig. 6. FE-SEM micrographs of fracture surfaces of ZT50 quenched specimens. (a) Specimen quenched from 1400 °C. The phase presenting transgranular fracture is TiO_2, the grains with intergranular fracture is t-ZrO_2 and the small grains observed at the boundaries of these grains can be associated with pyrochlore. (b) Specimen quenched from 1500 °C. It is not possible to distinguish the major phase (Figs. 4 and 7). Small angular grains of pyrochlore are observed.

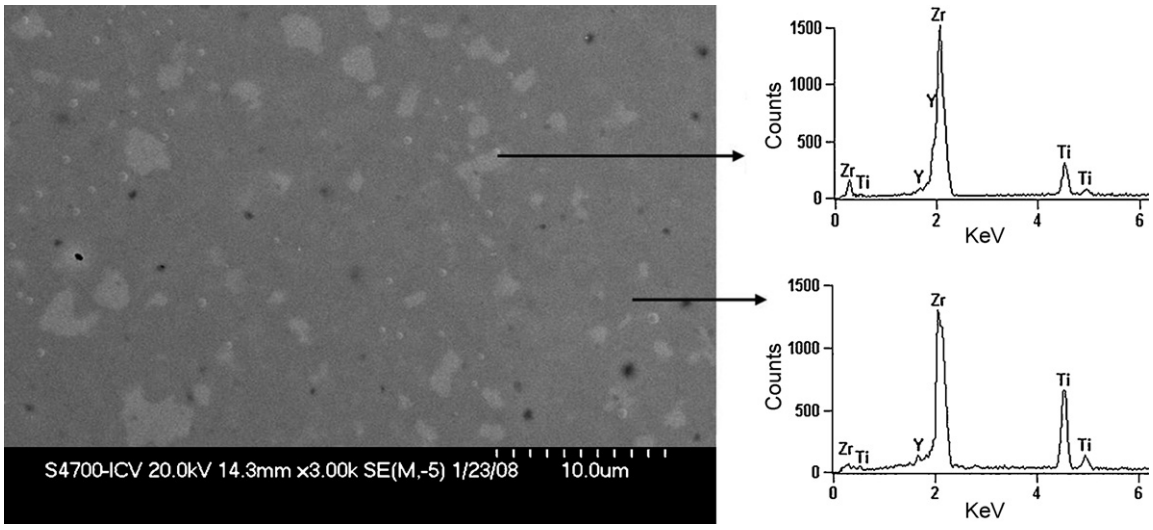

Fig. 7. Microstructure of ZT50 quenched from 1500 °C on heating. FE-SEM micrographs of polished surfaces, together with characteristic EDX analyses. Semi-quantitative analyses gave a major phase (≈62–64 wt.% ZrO_2, 34–36 wt.% TiO_2, 2–3 wt.% Y_2O_3) that could be identified as $ZrTiO_4$ss, meanwhile the white areas (≈68–70 wt.% ZrO_2, 17–20 wt.% TiO_2, 13–15 wt.% Y_2O_3) should correspond to c-ZrO_2 with a certain amount of TiO_2 and Y_2O_3 in solid solution.

Concentrated suspensions of Y-TZP (Z) and TiO_2 (T) were prepared separately to 45 vol.% solids by adding the powder to the proper amount of deionised water containing 0.8 wt.% of polyacrylic-based dispersant (Dolapix CE64, Zschimmer-Schwarz, Lahnstein, Germany) and further mixing with a high shear mixer (Silverson, L2R, Chesham, United Kingdom). Then, they were ball milled for 24 h using alumina jar and balls. The so-prepared one component suspensions were then mixed in a molar ratio 1:1 (i.e. 60.58 wt.% Z and 39.42 wt.% T) in order to obtain ZT50 materials. The resulting mixture was ball milled further for 1 h. Details of the preparation procedure are given in a previous work.[19]

The green bodies shaped into plates of 70 mm × 70 mm × 10 mm were prepared by slip casting the Z, T and ZT50 suspensions in plaster moulds and dried in air for 48 h. Specimens for the different tests were obtained by cutting these plates.

Constant heating rate (CHR, heating and cooling rates 5 °C/min) experiments up to 1600 °C were performed in a differential dilatometer with alumina rod (Adamel Lhomargy, DI24, Brie France) and in a differential thermal and thermogravimetric analyser (STA 409, Netzsch, Selb, Germany, DTA–TG). From the results of the dilatometer and DTA–TG analyses of ZT50, the temperatures of interest were selected (1400 and 1500 °C on heating and 1000 °C on cooling) and specimens were prepared by quenching from those temperatures. The experimental process to get the 1400 and 1500 °C quenched specimens consisted in heating at 5 °C/min to the final temperature, a dwell of 1 min at the maximum temperature and then quenching to room

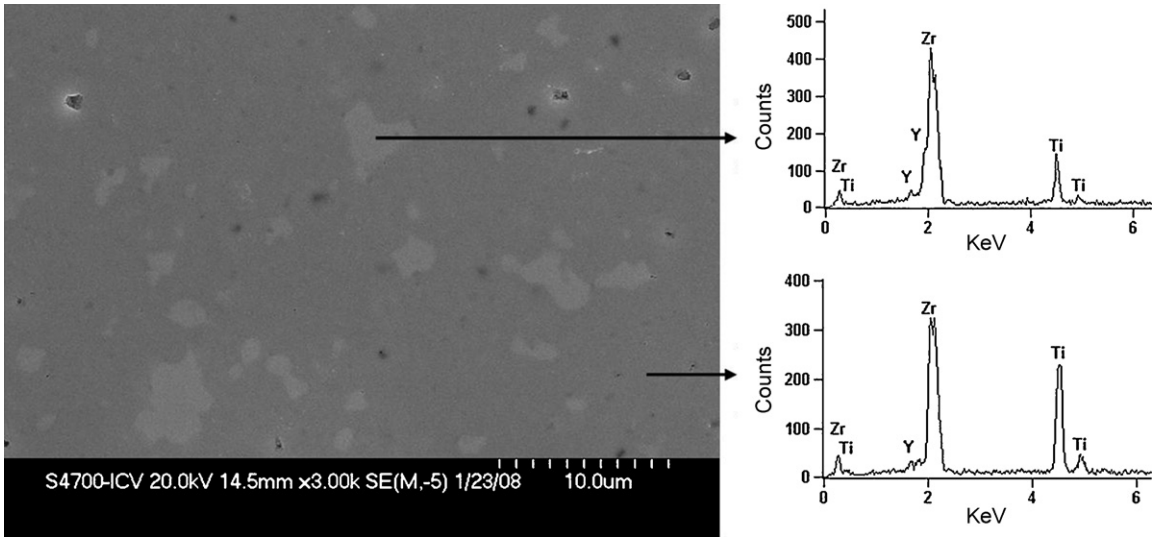

Fig. 8. Microstructure of ZT50 quenched from 1000 °C on cooling. FE-SEM micrographs of polished surfaces, together with characteristic EDX analyses. Semi-quantitative analyses gave a major phase (≈59–61 wt.% ZrO_2, 36–38 wt.% TiO_2, 1–2 wt.% Y_2O_3) that could be identified as $Zr_5Ti_7O_{24}$, meanwhile the white areas (≈68–71 wt.% ZrO_2, 16–18 wt.% TiO_2, 12–14 wt.% Y_2O_3) should correspond to c-ZrO_2 with a certain amount of TiO_2 and Y_2O_3 in solid solution.

temperature; the 1000 °C specimen was heated at 5 °C/min to 1500 °C where it was kept during 1 min before being cooled at 5 °C/min to 1000 °C where it was kept during 1 min before being quenched. Quenching was performed in air stream using a hair drier, this cooling method, traditionally used in phase equilibrium diagram building, assures cooling times from the treatment temperature to 800 °C of less than 1 min for the small (≈5 mm × 5 mm × 5 mm) specimens used.

The quenched specimens were characterized as pieces by X-ray diffraction (XRD) using a Siemens D5000 diffractometer (Munich, Germany) and Si as internal standard. The obtained XRD patterns were analysed using the diffraction files of $ZrTiO_4$ (ASTM 34-415), $Zr_5Ti_7O_{24}$ (ASTM 34-209), $Zr_{0.963}Y_{0.037}O_{1.982}$ (ASTM 83-113), r-TiO_2 (ASTM 21-1276), $Zr_{0.62}Y_{0.20}Ti_{0.18}O_{1.90}$[16] and Si (ASTM 77-2111).

The microstructures of diamond polished (down to 3 μm) samples were characterized by field emission gun-scanning electron microscopy with energy dispersive X-ray microanalysis (FE-SEM-EDX, Hitachi S-4700 type I, Tokyo, Japan). Additional FE-SEM characterization was done on fracture surfaces of materials quenched from 1400 and 1500 °C to complete the phase identification done on the polished specimens that did not allow the complete identification of existing phases.

Two materials named ZT501500 and ZT501500-30h were prepared using thermal treatments of 2 h and 30 h, respectively, at 1500 °C and the same heating and cooling rates (5 °C/min) and characterized by XRD and FE-SEM-EDX. The microstructural characterization by FE-SEM-EDX of these materials was carried out in polished (down to 3 μm) and thermally etched (1400 °C for 1 min, heating and cooling rates of 5 °C/min) surfaces. Additional characterization was done on fracture surfaces of these materials to assure the phase identification done on the polished and thermally etched specimens. Observations of un-etched polished surfaces did not allow the complete identification of existing phases.

Raman determinations of ZT501500 and ZT501500-30h on polished and thermally etched at 1400 °C specimens were performed in backscattering configuration at room temperature (RT) in a DILOR XY spectrometer (Lille, France) with a liquid-nitrogen cooled Charge-Coupled Device (CCD) detector and excitation through the 100× objective lens of a microscope (Olympus, BH2, Tokyo, Japan). To improve spatial resolution a confocal diaphragm was inserted at the laser path. With this setup spatial resolution was of about 1 μm. The 514.5 nm line of an Ar^+ laser was used as light source (Coherent, Innova 305C, Santa Clara, CA, USA).

3. Results and discussion

3.1. Reaction sintering process

Results from the CHR experiments are plotted in Figs. 1–3. No special features were observed in the shrinkage curve of Z (Fig. 1), accordingly, only one peak corresponding to the progressive sintering process was observed in the derivative one (Fig. 2); shrinkage started at ≈1100 °C and was arrested at ≈1550 °C. Conversely, the shrinkage curve of T (Fig. 1) showed

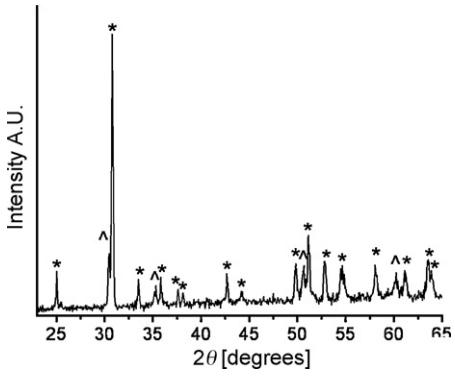

Fig. 9. X-ray diffraction pattern of the composites ZT50 sintered at 1500 °C/2 h. (*) $Zr_5Ti_7O_{24}$ and (∧) c-ZrO_2ss.

two significant slope changes that were highlighted in the derivative curve (Fig. 2). The first one, at intermediate temperatures, revealed a process occurring at about 1060 °C that accelerated shrinkage. This process can be identified as the transformation of anatase to rutile, which involves a sudden shrinkage of about 8.5 vol.% (calculated using the theoretical densities of anatase-TiO_2, 3.89 g/cm^3, and rutile-TiO_2, 4.25 g/cm^3, extracted from

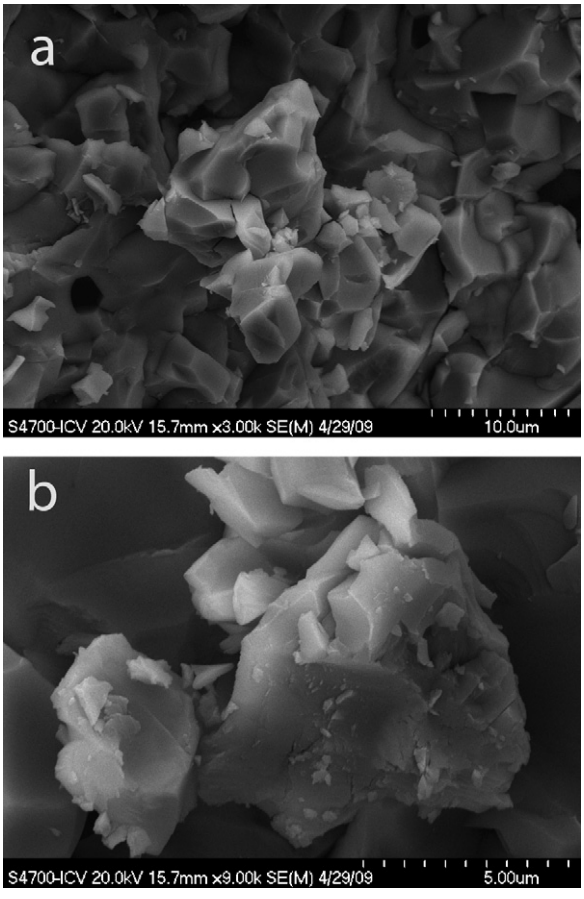

Fig. 10. Microstructure of the composite ZT50 sintered at 1500 °C/2 h. FE-SEM micrographs of fracture surfaces. The major phase, dark gray, presents transgranular fracture and was identified as $Zr_5Ti_7O_{24}$ (Fig. 11). The secondary phase, light gray, that presents intergranular fracture was identified as c-ZrO_2 (Fig. 11). Small grains surrounding this phase were identified as pyrochlore (Fig. 11).

ASTM files 21-1272 and 21-1276). This transformation occurs between 400 and 1200 °C depending on several parameters, such as grain size, impurities and atmosphere.[20–22] The second slope change (≈1220 °C) corresponded to maximum shrinkage rate and it was wider than the previous one indicating a progressive process, as in the case of Z. Shrinkage was arrested at ≈1400 °C for T.

The initiation of shrinkage of the mixture ZT50 (≈1000 °C) (Fig. 1), was significantly delayed with respect to that of T (≈900 °C) and started at slightly lower temperature than for Z (≈1100 °C). The shrinkage curve showed two slope changes at intermediate temperatures, which were also highlighted in the derivative curve (Fig. 3). For ZT50, the transformation of TiO_2 from anatase to rutile produced a sharp acceleration of shrinkage that occurred at a slightly higher temperature (≈1100 °C) than for T (≈1060 °C) and was less pronounced because of the smaller amount of TiO_2 in the ZT50 composition. The anatase–rutile transformation is not detected by DTA (Fig. 3) due to the low enthalpy change associated ($\Delta H^0_{971} = -0.78 \pm 0.20$ kcal mol^{-1}, according to calculations by Mitsuhashi and Kleppa[23]). For higher temperatures, shrinkage of ZT50 continued in a progressive way and was arrested at about 1440 °C, temperature at which a clear endothermic peak was observed in the DTA curve (Fig. 3). In principle, both features, the shrinkage arrest and the endothermic peak could be associated to the formation of the high temperature phase of zirconium titanate, $ZrTiO_4$, with a formation enthalpy of 11.64 kJ/mol at 1440 °C[3] and which formation from the reaction of tetragonal zirconia (density = 6.07 g/cm^3, ASTM 83-113) and rutile (density = 4.25 g/cm^3, ASTM 21-1276) is slightly expansive (≈2.4 vol.%). In order to analyse this process, 1400 and 1500 °C were selected as quenching temperatures.

The DTA curve registered during cooling (Fig. 3) showed an exothermic peak at ≈1150 °C, that would correspond to the transition between high-temperature form ($ZrTiO_4$) and low-temperature form ($Zr_5Ti_7O_{24}$)[9,11,24] of zirconium titanate. In order to analyse this process, samples treated up to 1500 °C and cooled down to 1000 °C were also selected for quenching.

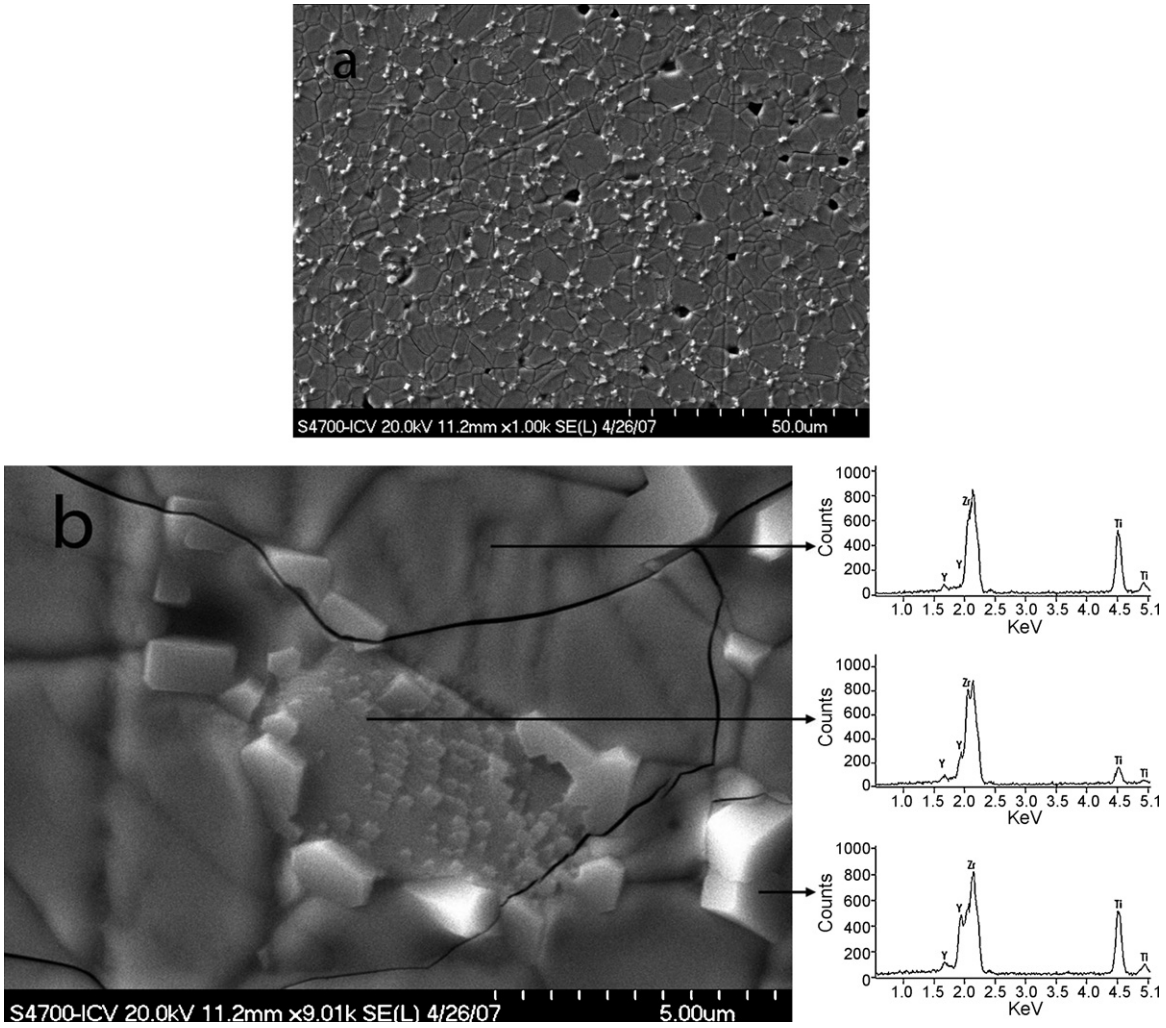

Fig. 11. Microstructure of the composites ZT50 sintered at 1500 °C/2 h. FE-SEM micrographs of polished and thermally etched (1400 °C/1 min) surfaces, together with characteristic EDX analyses. Semiquantitative analyses gave a major phase (≈53–57 wt.% ZrO_2, 41–43 wt.% TiO_2, 2–3 wt.% Y_2O_3) that could be identified as $Zr_5Ti_7O_{24}$, meanwhile the second phase (≈62–64 wt.% ZrO_2, 14–18 wt.% TiO_2, 19–23 wt.% Y_2O_3) should correspond to c-ZrO_2 with a certain amount of TiO_2 and Y_2O_3 in solid solution, and the minor third phase (≈40–45 wt.% ZrO_2, 27–33 wt.% TiO_2, 24–30 wt.% Y_2O_3) should be pyrochlore.

XRD patterns of the quenched samples are shown in Fig. 4 and SEM micrographs are shown in Figs. 5–8. In the specimens quenched from 1400 °C, the crystalline phases detected by XRD were rutile (r-TiO_2) and tetragonal zirconia (t-ZrO_2) (Fig. 4a), in agreement with the biphasic microstructure observed in the polished surfaces FE-SEM (Fig. 5), in which the two phases appeared highly interpenetrated. The semiquantitative analysis by EDX was not possible due to the small size of the areas occupied by the phases in the samples quenched from 1400 °C, nevertheless the EDX diagrams allowed to identify the gray coloured areas as TiO_2 and the white ones as ZrO_2 (Fig. 5). In agreement, the XRD patterns showed the t-ZrO_2 displaced towards higher angles with respect to the $Zr_{0.963}Y_{0.037}O_{1.982}$ pattern, which could be due to the solid solution of TiO_2 in t-ZrO_2. In the specimens quenched from 1400 °C, $ZrTiO_4$, equilibrium phase already at 1300 °C,[17] was not formed due to the short periods at 1300–1400 °C involved in the CHR experiments, as occurred in the work by Ananta et al.[8] that did not observe any significant process during CHR (10 °C/min) treatments up to 1400 °C. Even though the FE-SEM observations of polished surfaces and the XRD patterns corresponded to a biphasic material, additional observations of the fracture surfaces of specimens quenched from 1400 °C showed small particles located at the boundaries that corresponded to a minor third phase (Fig. 6a), as will be discussed after the Raman determinations.

The FE-SEM microstructure of the specimens quenched from 1500 °C (Fig. 7) and polished appeared also as biphasic. The semiquantitative EDX analyses of the major phase allowed associating it with $ZrTiO_4$. The peaks that would correspond to $ZrTiO_4$ in the XRD diagrams (Fig. 4) were clearly shifted towards angles higher than those of the $ZrTiO_4$ pattern. The possibility of solid solution of TiO_2 in $ZrTiO_4$ ($ZrTiO_4$ss) at 1500 °C was reported by several authors.[9,16–18] Thus, the gray major phase observed in the specimens quenched from 1500 °C could be unequivocally identified with $ZrTiO_4$ss. The EDX semiquantitative analysis of the white areas gave ZrO_2 with TiO_2 and Y_2O_3 in solid solution. The XRD peaks that would correspond to ZrO_2 in the specimens quenched from 1500 °C ($2\theta \approx 30.45°$, 35.25°, 50.65° and 60.1°, Fig. 4) were extremely shifted towards angles higher than those of t-ZrO_2 ($Zr_{0.963}Y_{0.037}O_{1.982}$, ASTM 83-113) and c-$ZrO_2$ ($Zr_{0.8}Y_{0.2}O_{1.9}$, ASTM 82-1246) XRD patterns and close to those of c-ZrO_2 with 11.4 wt.% of TiO_2 and 18.0 wt.% of Y_2O_3 in solid solution reported by Feighery et al.[16] Other authors[15] have also reported the existence of a solid solution of TiO_2 (up to 11.8 wt.%) and Y_2O_3 (up to 12.2 wt.%) in c-ZrO_2 at 1500 °C. Moreover, the above mentioned peaks were shifted about 0.2° towards angles higher than those reported by Feighery et al.[16] which would indicate a higher amount of ions with smaller ionic radius than that of Zr^{4+} ($R_i = 0.80$ Å),[25] such as Ti^{4+} ($R_i = 0.68$ Å),[25] and/or a lower amount of ions with larger ionic radius than that of Zr^{4+}, such as Y^{3+} ($R_i = 0.93$ Å),[25] in agreement with the semiquantitative composition of the white grains (Fig. 7). The presence of c-ZrO_2ss in the specimens quenched from 1500 °C supports the phase relationships proposed by Schaedler et al.[17] in the isothermal section at 1500 °C. As occurred for the specimens quenched from 1400 °C, a minor third phase appeared in the fracture surfaces of these specimens.

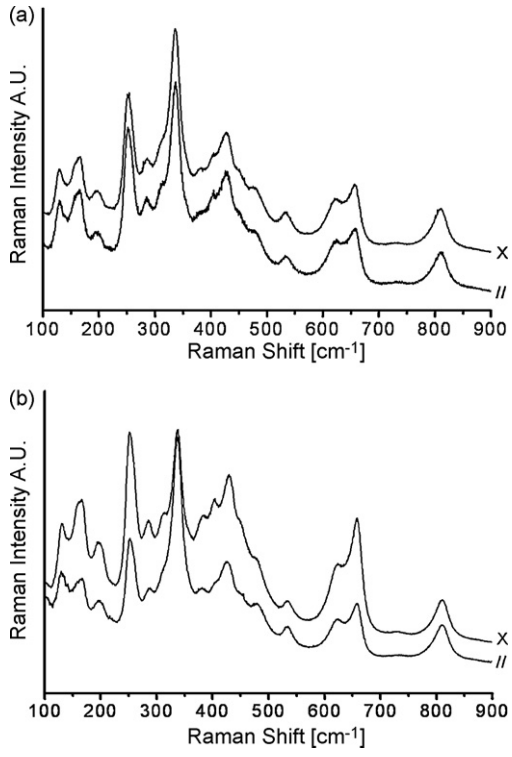

Fig. 12. Raman spectra of composites ZT50 sintered at 1500 °C/2 h. (a) Spectra of the major phase ($Zr_5Ti_7O_{24}$) and (b) spectra of the microcrystals of the minor third phase. (× crossed configuration, // parallel configuration).

In this case the amount of third phase particles was higher and they appeared surrounding the c-ZrO_2ss grains (Fig. 6b) as will be discussed after the Raman determinations.

In the microstructure of polished samples quenched from 1000 °C during the cooling part of the cycle major (gray) and minor (white) phases of similar compositions as those of specimens quenched from 1500 °C were detected (Fig. 8). From the XRD patterns (Fig. 4), the white secondary phase could also be identified as c-ZrO_2ss. The main difference between XRD spectra of the specimens quenched from 1500 and 1000 °C on cooling was the position of the peaks of zirconium titanate (Fig. 4), that were shifted to higher angles, corresponding to those of the low-temperature form of zirconium titanate, $Zr_5Ti_7O_{24}$ (ASTM 34-209).

3.2. Materials

Summarizing the above results, the reaction sintering process of equimolar mixtures of TiO_2 and ZrO_2 stabilized with 3 mol% of Y_2O_3 using relatively low heating and cooling rates (5 °C/min) would produce materials constituted by $Zr_5Ti_7O_{24}$ as major phase when temperatures higher than 1440 °C are used. On this basis, the selected temperature for the isothermal treatment to get a zirconium titanate based material was 1500 °C.

The density of the material sintered at 1500 °C during 2 h (ZT501500) was 5.02 ± 0.01 g/cm^3. The XRD pattern of ZT501500 (Fig. 9) shows a biphasic material constituted by $Zr_5Ti_7O_{24}$ as major phase and c-ZrO_2ss as second phase. It was not possible to characterize the microstructure of this material

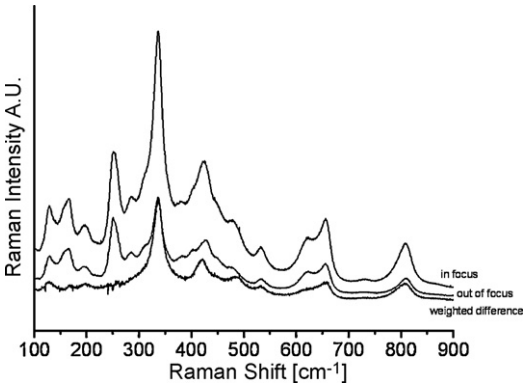

Fig. 13. Raman spectra in focus, out-of-focus and weighted difference, of the microcrystals of the minor third phase in composites ZT50 sintered at 1500 °C/2 h.

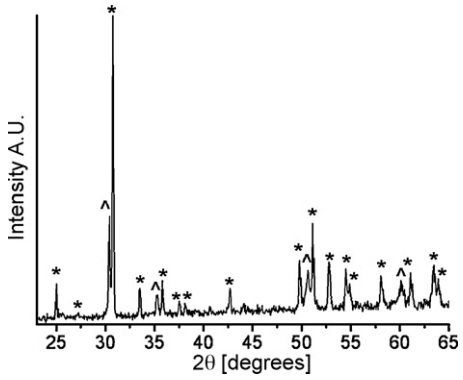

Fig. 14. X-ray diffraction pattern of the composites ZT50 sintered at 1500 °C/30 h. (*) $Zr_5Ti_7O_{24}$ and (∧) c-ZrO_2ss.

on un-etched polished surfaces. In the fracture surfaces shown in Fig. 10 three kinds of grains are observed. The largest and darkest ones presented transgranular fracture and constituted the major part of the surface (Fig. 10a). The smaller and clearer grains presented the characteristic facets of intergranular fracture (Fig. 10). These latter were surrounded by small (<2 μm) clear gray grains also surrounded by the fracture (Fig. 10b). These observations show that ZT501500 was constituted by three phases.

In order to reveal the grains of the phases in the polished surfaces, a very short (1 min) thermal etching at high temperature was performed; the obtained microstructure is shown in Fig. 11. The major phase with dark gray colour in the FE-SEM images (Figs. 10a and 11) and zirconium titanate composition (Fig. 11b) could be identified as the $Zr_5Ti_7O_{24}$ observed by XRD (Fig. 9). The second phase formed by relatively large grains (≈3–5 μm), clearer in the FE-SEM images (Figs. 10a and 11), was identified with c-ZrO_2ss, in agreement with its composition and the XRD pattern of the material. The minor third phase constituted by small (<2 μm) white grains that was found surrounding the c-ZrO_2ss grains in the fracture surfaces (Fig. 10b) was clearly revealed by the thermal etching (Fig. 11). Semiquantitative analysis by EDX (Fig. 11b) showed that this minor phase was Y_2O_3-richer than the major ones. In order to clarify the nature of this phase, Raman measurements were performed. Due to the triphasic character of this material, spectra were recorded by focusing the laser either into the major phase, identified as $Zr_5Ti_7O_{24}$, or onto the second phase, identified as a c-ZrO_2ss. The microcrystals of the minor third phase appearing at the boundary of the second phase grains could be seen through the optical microscope of the Raman spectrometer. However, their size was too small to be sure that the spectrum came from only one of such microcrystals. Even inserting a confocal diaphragm to limit the field depth, the scattering volume collected was much larger than the microcrystal. Thus, the identification could only be performed by indirect means.

Fig. 12 shows the Raman spectra of the material sintered at 1500 °C 2 h (ZT501500). The spectrum of the major phase (Fig. 12a) corresponded to that of $Zr_5Ti_7O_{24}$[26] and was unpolarized, in agreement with the expected depolarization of light in polycrystalline samples. When the laser was focused at the separation between the major and the second phases, where the microcrystals of the minor third phase were located, the spectrum (Fig. 12b) presented several differences compared to that of the matrix (Fig. 12a). The most important was the appearance of clear polarization rules, which implies that the laser was impinging on a single crystal area. However, the band positions and general aspect of the spectrum were very similar to that of the major phase ($Zr_5Ti_7O_{24}$) (Fig. 12a), except for minor frequency shifts in the region of 400 cm^{-1}.

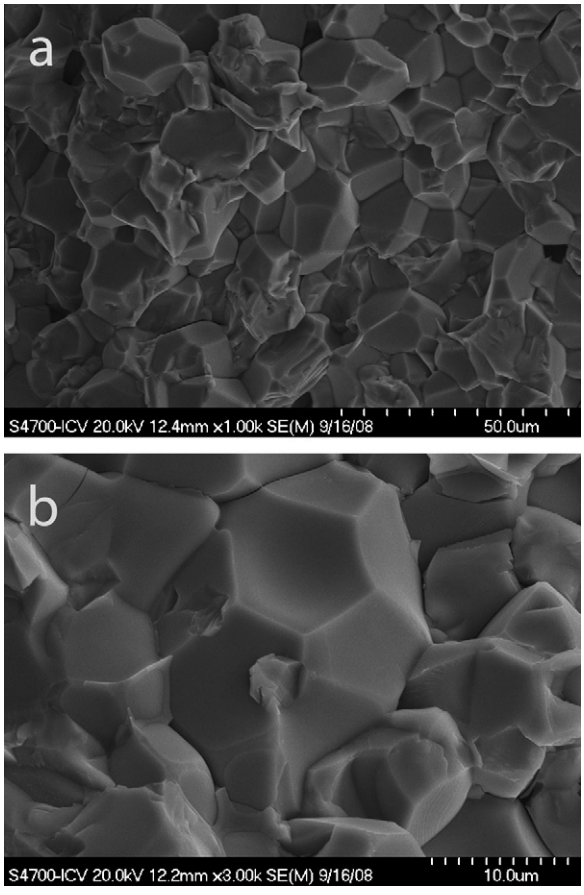

Fig. 15. Microstructure of the composite ZT50 treated at 1500 °C/30 h. FE-SEM micrographs of fracture surfaces. The phase that presents transgranular fracture was identified as $Zr_5Ti_7O_{24}$ (Fig. 16). The grains that present intergranular fracture were identified as c-ZrO_2 (Fig. 16).

A spectrum of a microcrystal of the minor third phase was tried to isolate through the following procedure (Fig. 13). Firstly, an area with large concentration of microcrystals was identified, and the laser was focused just at the surface of the material, so that the spectrum measured in that condition had maximum intensity. Strong polarization properties were found, indicating that the contribution of the microcrystals was important. Then, the sample holder was moved downward by steps, setting the laser out of focus and thus collecting a much wider area than in the optimal conditions. The spectrum resembled more and more that of the major phase ($Zr_5Ti_7O_{24}$), and polarization disappeared. The spectrum coming from the microcrystals was obtained by subtracting, with the appropriate factors, the out-of-focus spectrum from the optimal one. In that way, a very simple spectrum with high intensity in the 330 cm^{-1} region was obtained (Fig. 13). This region is typical of many Ti pyrochlores, though at slightly higher frequency.[27] The compositions of the regions containing the microcrystals (Fig. 11) would further support the microcrystals to be formed by Ti pyrochlores as suggested by the results of the Raman analyses.

The experimental isothermal section at 1500 °C reported by Schaedler et al.[17] shows that pyrochlore and zirconium titanate are not compatible, being c-ZrO_2 and zirconium titanate the compatible phases at 1500 °C. On the contrary, Feighery et al.[16] reported a isothermal section where pyrochlore and zirconium titanate are compatible at 1500 °C. In order to verify whether pyrochlore is an equilibrium phase at 1500 °C in the composition studied here, additional specimens were fabricated by sintering at 1500 °C during 30 h; the density of these specimens (ZT501500-30h) was 4.94 ± 0.05 g/cm^3. The two crystalline phases, $Zr_5Ti_7O_{24}$ and c-ZrO_2ss were identified by XRD (Fig. 14) in this material. FE-SEM observations on fracture surfaces (Fig. 15) and polished and thermally etched surfaces (Fig. 16) of this material, did not allow to discern any minor phase surrounding the c-ZrO_2ss grains like in the material ZT501500 (Figs. 10 and 11), which would indicate that pyrochlore is not an equilibrium phase at 1500 °C, in agreement

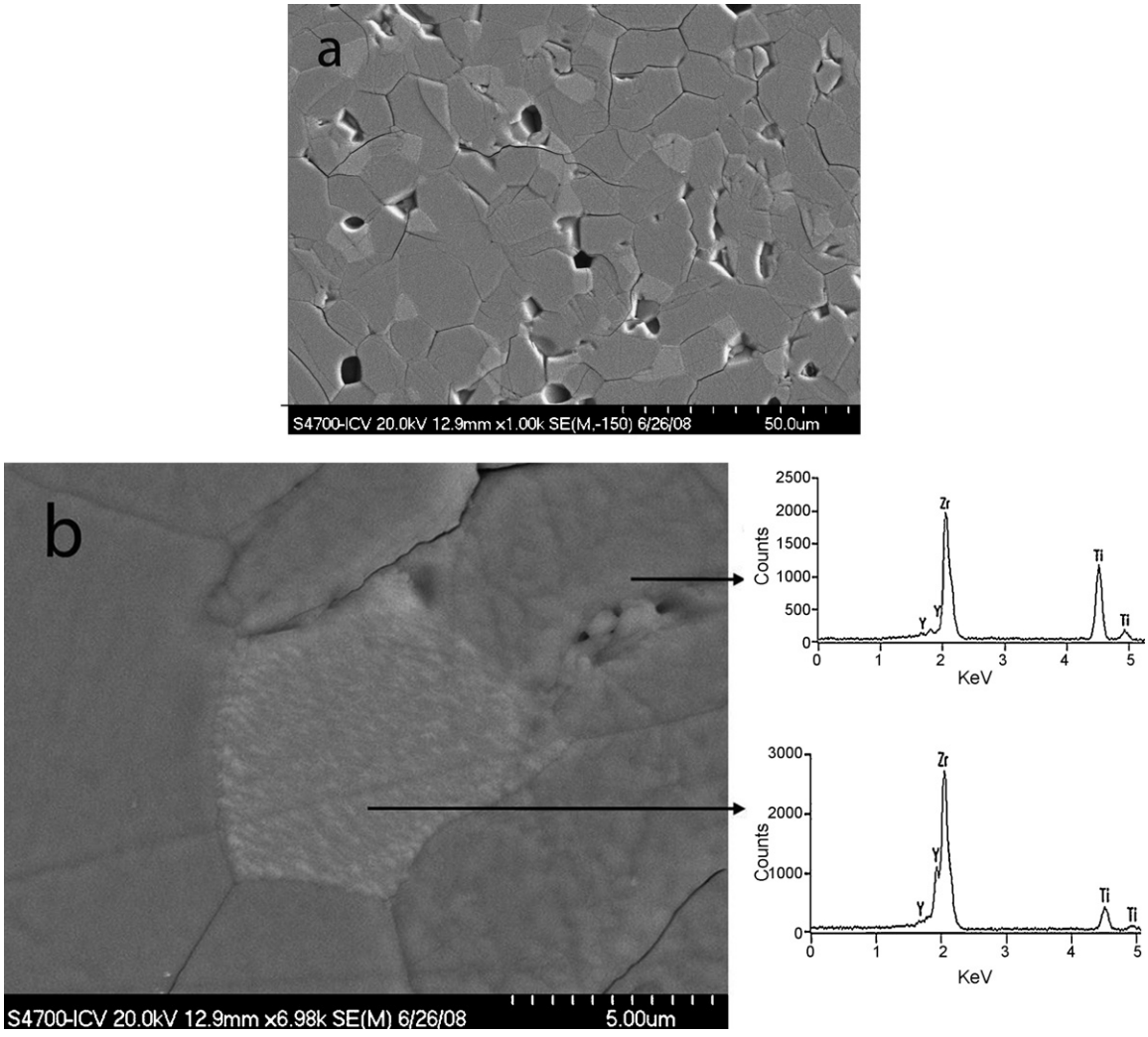

Fig. 16. Microstructure of the composites ZT50 sintered at 1500 °C/30 h. FE-SEM micrographs of polished and thermally etched (1400 °C/1 min) surfaces, together with characteristic EDX analyses. Semiquantitative analyses gave a major phase (≈61–63 wt.% ZrO_2, 33–35 wt.% TiO_2, 1–3 wt.% Y_2O_3) that could be identified as $Zr_5Ti_7O_{24}$, meanwhile the second phase (≈64–66 wt.% ZrO_2, 10–12 wt.% TiO_2, 23–25 wt.% Y_2O_3) should correspond to c-ZrO_2 with a certain amount of TiO_2 and Y_2O_3 in solid solution.

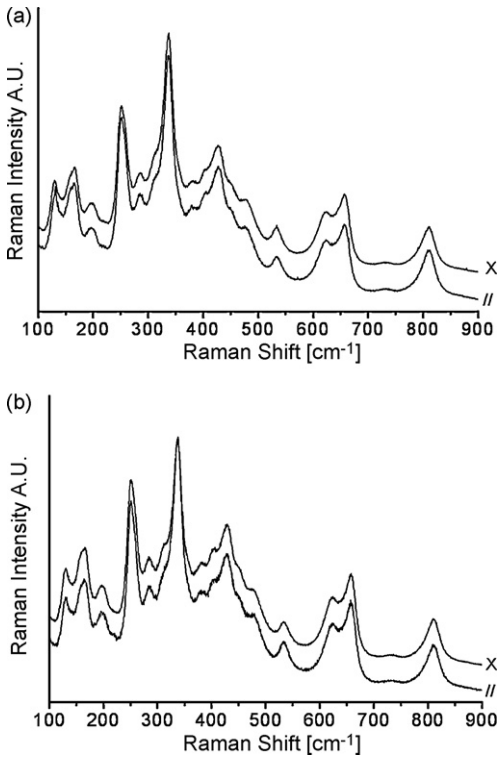

Fig. 17. Raman spectra of composites ZT50 sintered at 1500 °C/30 h. (a) Spectra of the major phase ($Zr_5Ti_7O_{24}$); (b) spectra of the boundary of the second phase (× crossed configuration, // parallel configuration).

with the Raman observations discussed below and the results of Schaedler et al.[17] Fig. 17 shows Raman spectra of the material treated at 1500 °C for 30 h (ZT501500-30h). The spectrum of the major phase showed no polarization and, as in the material annealed for 2 h, corresponded to $Zr_5Ti_7O_{24}$. The spectrum of the boundary between the major and the second phase showed some polarization degree, but it was much weaker than in the material annealed for 2 h. Thus, if microcrystals of the minor third phase were present in material annealed for 30 h, they had a negligible contribution in terms of volume content.

One final aspect to comment about Raman measurements is the total impossibility to detect a spectrum that could be assigned to tetragonal or cubic zirconia in these materials. In the case of t-ZrO_2, the non-detection of its spectrum means that this phase was not present in these materials, since it is a very active Raman scatterer. The situation with c-ZrO_2ss is different, since this phase is only formed by extensive doping, which makes it very defective. Its spectrum, in consequence, is weak and presents very broad bands which might be difficult to detect if they were overlapped with another intense spectrum as in the case of $Zr_5Ti_7O_{24}$. This situation might be more complicated if c-ZrO_2 phase contains a large amount of TiO_2 and Y_2O_3 in solid solution as in ZT501500 and ZT501500-30h materials.

From the above discussion, it is clear that the pyrochlore particles observed surrounding the c-ZrO_2ss grains in the material treated at 1500 °C during 2 h are metastable. However, small pyrochlore particles were clearly observed surrounding the zirconia grains in the specimens quenched from 1500 °C and at some grain boundaries in the specimens quenched from 1400 °C (Fig. 6), which shows that pyrochlore was formed during the heating treatment up to 1500 °C. This fact can be explained by the extremely low Gibbs free energy of formation of pyrochlore (−4593 kJ/mol at 1000 °C and −4918 kJ/mol at 1500 °C using the function given by Schaedler et al.[17]). It will be easily formed at the grain boundaries between zirconia and titania, even before the reaction of these compounds to form zirconium titanate, with a higher Gibbs free energy in the whole range of temperatures considered (−2292 kJ/mol at 1000 °C and −2464 kJ/mol at 1500 °C using the function given by Schaedler et al.[17]). Therefore, pyrochlore formed at the grain boundaries of the material studied here during the heating up of the specimens and even at the initial part of the isothermal treatment at 1500 °C, as observed in the specimens quenched from 1400 and 1500 °C (Fig. 6) and treated at 1500 °C during 2 h (Figs. 10 and 11). Longer times at 1500 °C will allow the progressive reaction of pyrochlore and zirconium titanate to form c-ZrO_2ss and r-TiO_2, reaction which is favourable at 1500 °C.[17] In fact, an increase in the amount of c-ZrO_2ss for the sample treated during 30 h is qualitatively observed when a comparison between the XRD relative height of the (1 1 1) peak ($2\theta \approx 30.45°$) of c-ZrO_2ss and the (1 3 1) peak ($2\theta \approx 30.76°$) of $Zr_5Ti_7O_{24}$ of the samples treated 2 h (≈0.22) and 30 h (≈0.35) are compared. The excess r-TiO_2 produced in this reaction could enter in the structure of $ZrTiO_4$ss during cooling to form the low-temperature form $Zr_5Ti_7O_{24}$, or in c-ZrO_2ss.

4. Conclusions

The reaction sintering process of equimolar mixtures of TiO_2 and ZrO_2 stabilized by 3 mol% of Y_2O_3 to get zirconium titanate based materials, using relatively low heating and cooling rates (5 °C/min) and 1500 °C as maximum temperature, has been studied.

During the heating part of the cycle $ZrTiO_4$ is formed at ≈1440 °C. On cooling, the transition between $ZrTiO_4$ and $Zr_5Ti_7O_{24}$ occurs at ≈1150 °C.

Materials sintered at 1500 °C/2 h are constituted by $Zr_5Ti_7O_{24}$ as major phase, a solid solution of TiO_2 and Y_2O_3 in c-ZrO_2, and pyrochlore as minor phase. The presence of the pyrochlore phase can be explained considering the short soaking time of the thermal treatment employed in this work (2 h) since it is not an equilibrium phase at 1500 °C.

Acknowledgements

This work has been supported by the Spanish Ministry of Education and Science under contracts MEC MAT2006-13480 C02-01 and MAT2007-64486 C07-02. E. López-López acknowledges to Community of Madrid (Spain) and European Social Fund for economical support by CPI/0552/2007 contract.

References

1. Ikawa H, Iwai A, Iruta K, Shimojima H, Urabe K, Udagawa S. Phase transformation and thermal expansion of zirconium and hafnium titanates and their solid solutions. *J Am Ceram Soc* 1988;**71**:120–7.

2. Bhattacharya AK, Mallick KK, Hartridge A, Woodhead JL. Sol gel preparation, structure and thermal stability of crystalline zirconium titanate microspheres. *J Mater Sci* 1996;**31**:267–71.
3. Hom BK, Stevens R, Woodfield BF, Boerio-Goates J, Putnam L, Helean KB, et al. The thermodynamics of formation, molar heat capacity, and thermodynamic functions of $ZrTiO_4$(cr). *J Chem Thermodyn* 2001;**33**:165–78.
4. Christoffersen R, Davies PK. Extended defect intergrowths in $Zr_{1-x}Ti_{1+x}O_4$. *Solid State Ionics* 1992;**57**:59–69.
5. Kim IJ, Kim HC. Zero level thermal expansion materials based on $ZrTiO_4$–Al_2TiO_5 ceramics synthesized by reaction sintering. *J Ceram Proc Res* 2004;**5**:308–12.
6. Vittayakorn N. Synthesis and a crystal structural study of microwave dielectric zirconium titanate ($ZrTiO_4$) powders via a mixed oxide synthesis route. *J Ceram Proc Res* 2006;**7**:288–91.
7. Licina V, Gajovic A, Mogus-Milankovic A, Djerdj I, Tomasic N, Su D. Correlation between the microstructure and the electrical properties of $ZrTiO_4$ ceramics. *J Am Ceram Soc* 2008;**91**:178–86.
8. Ananta S, Tipakontitikul R, Tunkasiri T. Synthesis, formation and characterization of zirconium titanate (ZT) powders. *Mater Lett* 2003;**57**:2637–42.
9. McHale AE, Roth RS. Low-temperature phase relationships in the system ZrO_2–TiO_2. *J Am Ceram Soc* 1986;**69**:827–32.
10. Troitzsch U, Ellis DJ. The ZrO_2–TiO_2 phase diagram. *J Mater Sci* 2005;**40**:4571–7.
11. Bordet P, McHale A, Santoro A, Roth RS. Powder neutron diffraction study of $ZrTiO_4$, $Zr_5Ti_7O_{24}$ and $FeNb_2O_6$. *J Solid State Chem* 1986;**64**:30–46.
12. Azough F, Wright A, Freer R. The microstructure and dielectric properties of $Zr_5Ti_7O_{24}$ ceramics. *J Solid State Chem* 1994;**108**:284–90.
13. Wang CL, Lee HY, Azough F, Freer R. The microstructure and microwave dielectric properties of zirconium titanate ceramics in the solid solution system $ZrTiO_4$–$Zr_5Ti_7O_{24}$. *J Mater Sci* 1997;**32**:1693–701.
14. Fagg DP, Frade JR, Mogensen M, Irvine JTS. Effects of firing schedule on solubility limits and transport properties of ZrO_2–TiO_2–Y_2O_3 fluorites. *J Solid State Chem* 2007;**180**:2371–6.
15. Colomer MT, Durán P, Caballero A, Jurado JR. Microstructure, electrical properties and phase equilibria relationships in the ZrO_2–Y_2O_3–TiO_2 system: the subsolidus isothermal section at 1500 °C. *Mater Sci Eng A* 1997;**229**:114–22.
16. Feighery AJ, Irvine JTS, Fagg DP, Kaiser A. Phase relations at 1500 °C in the ternary system ZrO_2–Y_2O_3–TiO_2. *J Solid State Chem* 1999;**143**:273–6.
17. Schaedler TA, Fabrichnaya O, Levi CG. Phase equilibria in the TiO_2–$YO_{1.5}$–ZrO_2 system. *J Eur Ceram Soc* 2008;**28**:2509–20.
18. Kobayashi K, Kato K, Terabe K, Yamaguchi S, Iguchi Y. Phase relation of ZrO_2–$YO_{1.5}$–TiO_2 ceramic prepared by sol–gel method. *J Ceram Soc Jpn* 1998;**106**:860–6.
19. López-López E, Baudín C, Moreno R. Synthesis of zirconium titanate based materials by colloidal filtration and reaction sintering. *Int J Appl Ceram Technol* 2008;**5**:394–400.
20. Shannon RD, Pask JA. Kinetics of the anatase–rutile transformation. *J Am Ceram Soc* 1965;**48**:391–8.
21. Gouma PI, Mills MJ. Anatase-to-rutile transformation in titania powders. *J Am Ceram Soc* 2001;**84**:619–22.
22. Iida Y, Ozaki S. Grain growth and phase transformation of titanium oxide during calcination. *J Am Ceram Soc* 1961;**44**:120–7.
23. Mitsuhashi T, Kleppa OJ. Transformation enthalpies of the TiO_2 polymorphs. *J Am Ceram Soc* 1979;**62**:356–7.
24. McHale AE, Roth RS. Investigation of the phase transition in $ZrTiO_4$ and $ZrTiO_4$–SnO_2 solid solutions. *J Am Ceram Soc* 1983;**66**:C18.
25. Cotton FA, Wilkinson G. Non molecular solids. In: *Advanced Inorganic Chemistry.* Mexico: Limusa; 1996. p. 31.
26. Azough F, Freer R, Petzelt J. A Raman spectral characterization of ceramics in the system ZrO_2–TiO_2. *J Mater Sci* 1993;**28**:2273–6.
27. Glerup M, Nielsen OF, Poulsen FW. The structural transformation from the pyrochlore structure, $A_2B_2O_7$, to the fluorite structure, AO_2, studied by Raman spectroscopy and defect chemistry modeling. *J Solid State Chem* 2001;**160**:25–32.